

# Supporting Information

## Parasitic Reactions in Nanosized Silicon Anodes for Lithium-Ion Batteries

Han Gao<sup>1</sup>, Lisong Xiao<sup>2</sup>, Ingo Plümel<sup>2</sup>, Gui-Liang Xu<sup>1</sup>, Yang Ren<sup>3</sup>, Xiaobing Zuo<sup>3</sup>, Yuzi Liu<sup>4</sup>,

Christof Schulz<sup>2,5</sup>, Hartmut Wiggers<sup>2,5</sup>, Khalil Amine<sup>1\*</sup> and Zonghai Chen<sup>1\*</sup>

<sup>1</sup>Chemical Science and Engineering Division, Argonne National Laboratory, Lemont, IL, USA,  
60439

<sup>2</sup>Institute for Combustion and Gas Dynamics–Reactive Fluids (IVG), University of Duisburg-  
Essen, Duisburg, Germany, 47057

<sup>3</sup>X-ray Science Division, Advanced Photon Source, Argonne National Laboratory, Lemont, IL,  
USA, 60439

<sup>4</sup>Center for Nanoscale Materials, Argonne National Laboratory, Lemont, IL, USA, 60439

<sup>5</sup>Center for Nanointegration Duisburg-Essen (CENIDE), University of Duisburg-Essen,  
Duisburg, Germany, 47057

\* K. Amine: amine@anl.gov

\* Z. Chen: zonghai.chen@anl.gov



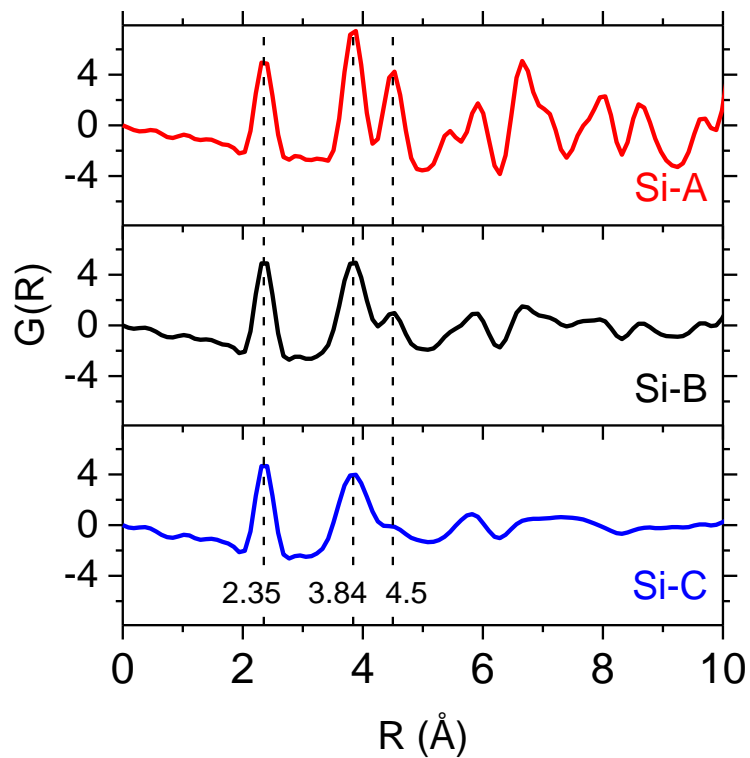


**Figure S1.** Pair distribution functions of Si-A, Si-B, and Si-C. The dashed lines correspond to the 1<sup>st</sup>, 2<sup>nd</sup>, and 3<sup>rd</sup> coordination shell Si-Si distances in a Si diamond matrix.

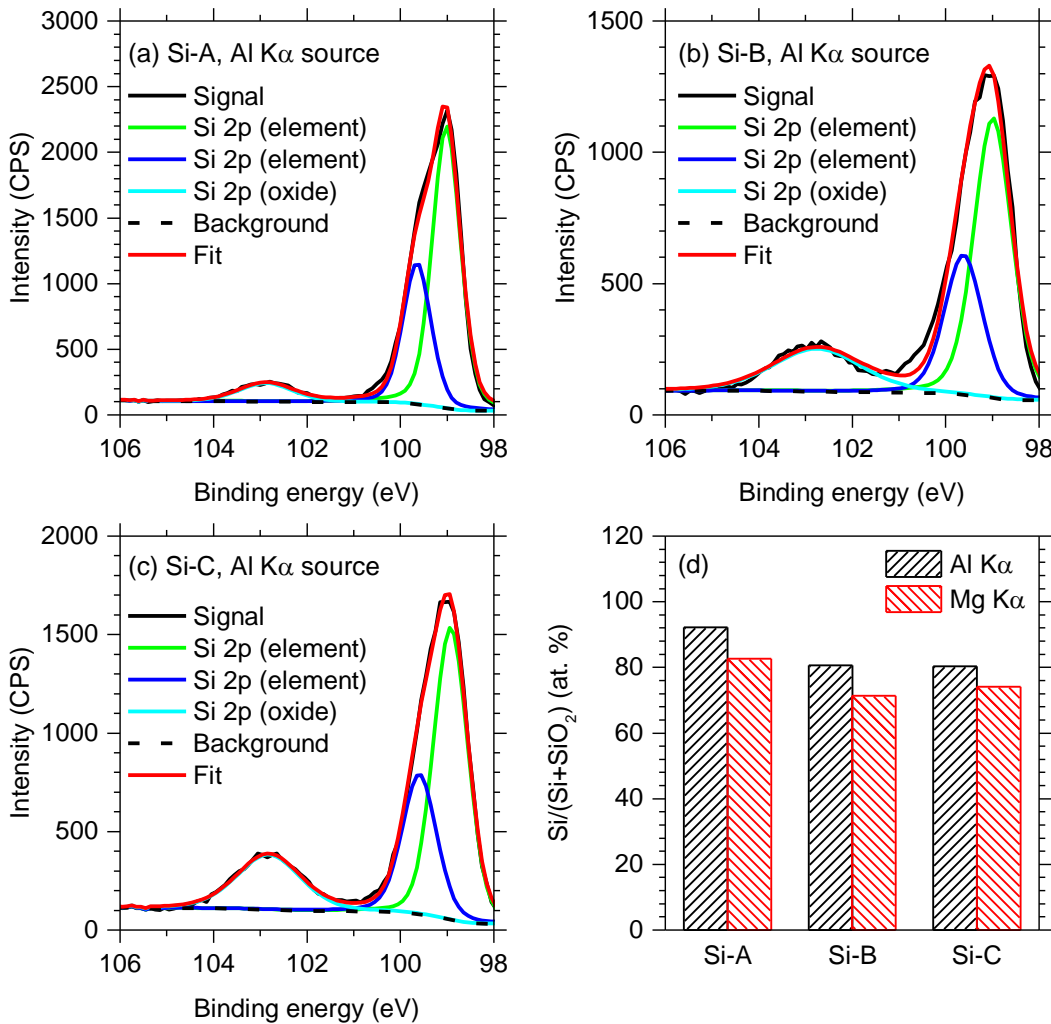


**Figure S2.** X-ray photoelectron spectra of the three Si NPs after a short exposure to air during the electrode-making process. The measured Si/(Si+SiO<sub>2</sub>) ratio is slightly lower when using the Mg K $\alpha$  source, which is not surprising as the Mg K $\alpha$  radiation is more surface sensitive due to its lower photon energy. The high values of the Si/(Si+SiO<sub>2</sub>) ratio indicate that the majority signals are mostly related to elemental Si. As a result the thickness of the native oxide layer must be very thin. Based on the effective electron escape depth of Si 2p in Si ( $\sim$ 15 Å),<sup>1</sup> the native oxide layer must be thinner than 15 Å as otherwise the Si 2p signal in elemental Si cannot be detected.

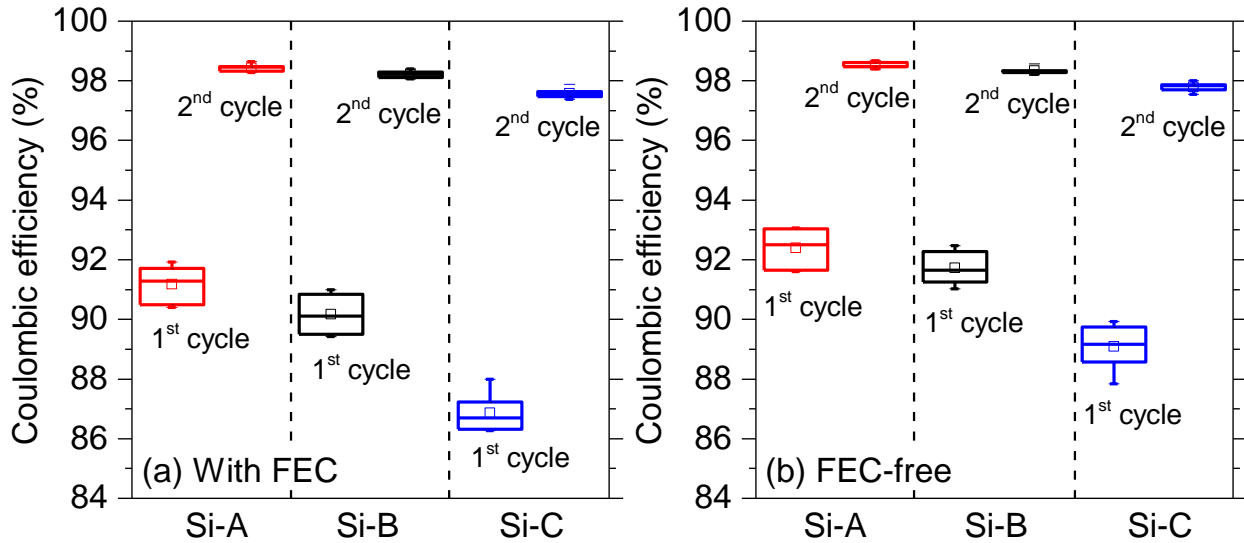


**Figure S3.** The box plots distributions of the 1<sup>st</sup> and 2<sup>nd</sup> cycle Coulombic efficiency of Si NP/Li half cells (a) with FEC additive and (b) without FEC additive (at least 10 cells in each category, the “whiskers” above and below the rectangle shows the maximum and minimum values while the small box and a segment inside the rectangle represents the average value and median value, respectively).

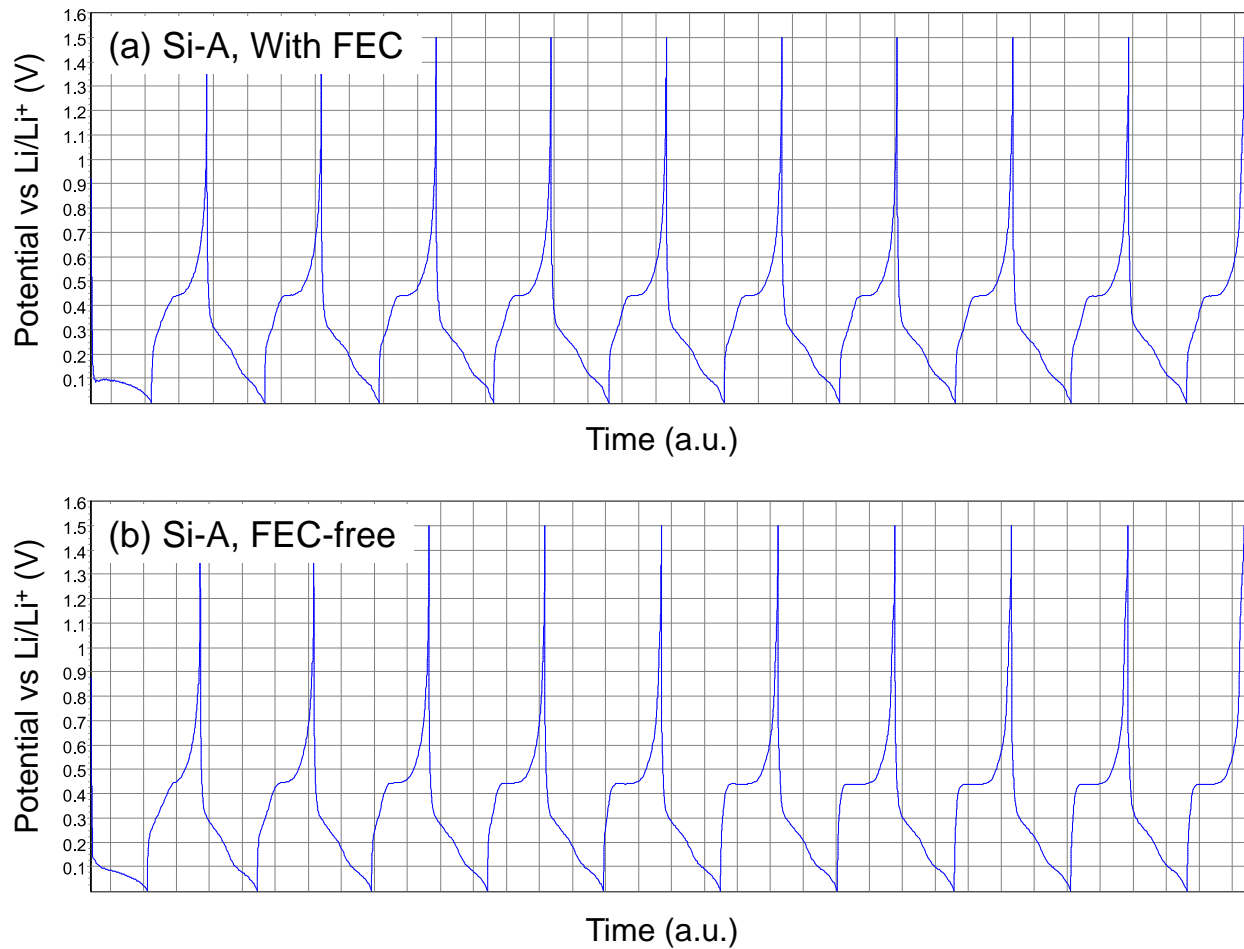


**Figure S4.** Discharge-charge profiles of Si-A/Li half cells using (a) electrolyte with FEC; and (b) electrolyte without FEC at a C-rate of 0.1.

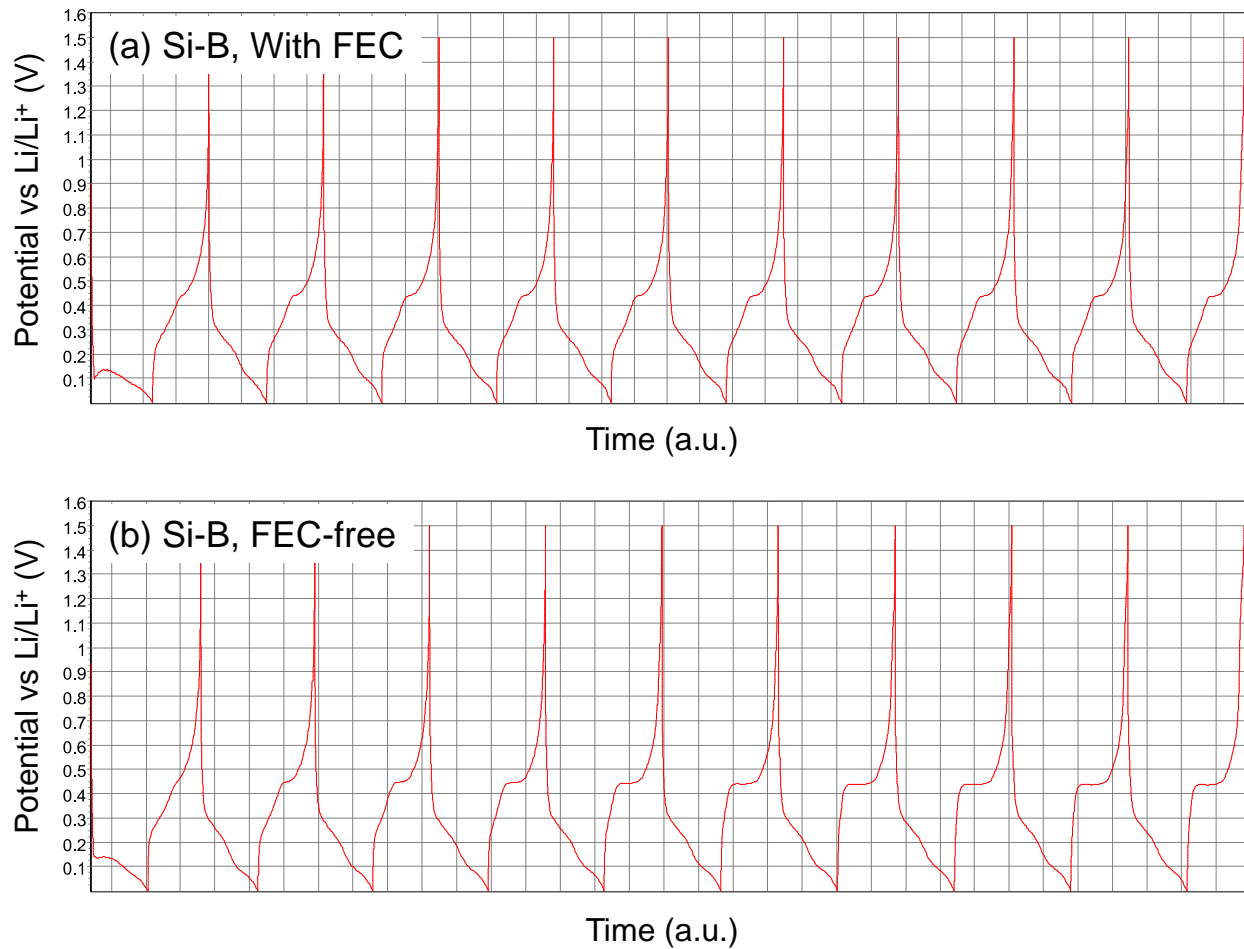


**Figure S5.** Discharge-charge profiles of Si-B/Li half cells using (a) electrolyte with FEC; and (b) electrolyte without FEC at a C-rate of 0.1.

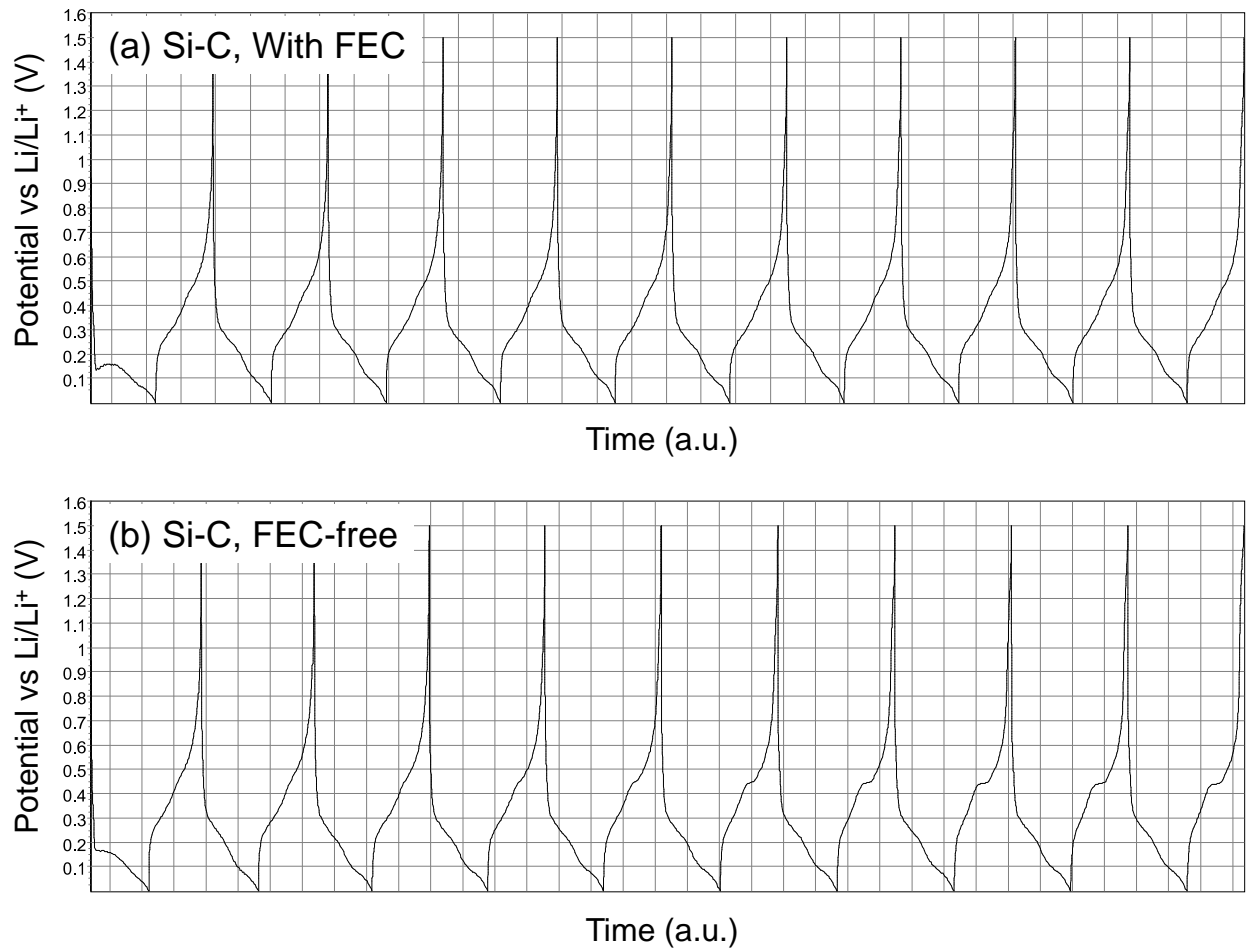


**Figure S6.** Discharge-charge profiles of Si-C/Li half cells using (a) electrolyte with FEC; and (b) electrolyte without FEC at a C-rate of 0.1.

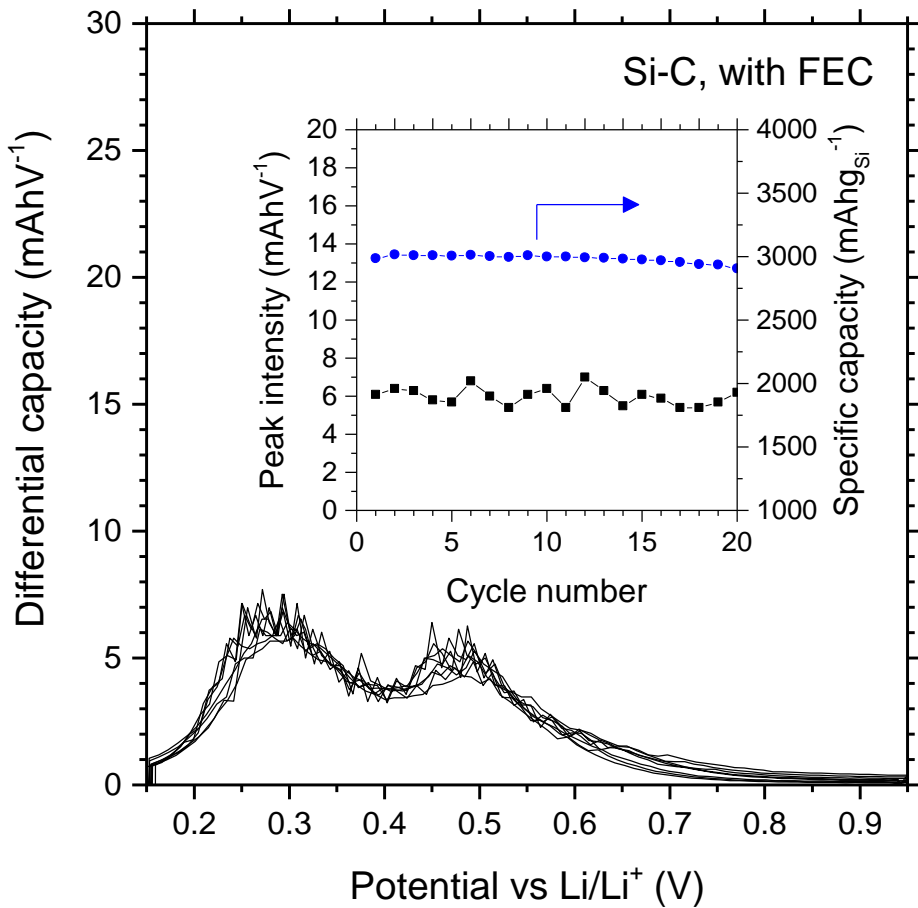


**Figure S7.** Evolution of differential capacity ( $dQ/dV$ ) plot of the Si-C NP/Li half cell during cycling under 0.1 C rate with FEC (inset shows the specific charge capacity as well as the intensity of the c- $\text{Li}_{15}\text{Si}_4$  peak at 0.45 V vs.  $\text{Li}/\text{Li}^+$  as a function of cycle number).

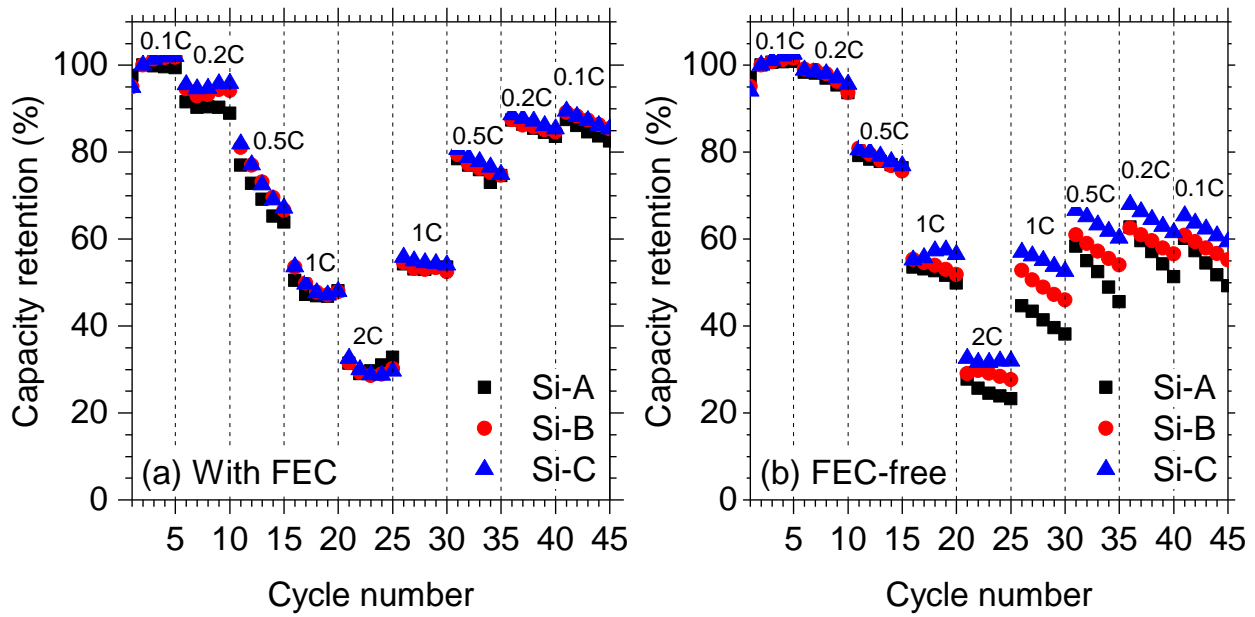


**Figure S8.** Rate performance of the three Si NP electrodes in the (a) electrolyte with FEC and (b) electrolyte without FEC (capacity normalized against the 2<sup>nd</sup> charge capacity at 0.1 C rate). The addition of FEC greatly improves the capacity retention over cycling. Very little amount of capacity loss was observed in the FEC-containing electrolyte after the rate tests while all three Si samples showed serious capacity loss (higher loss with larger Si particles) without the FEC additive.

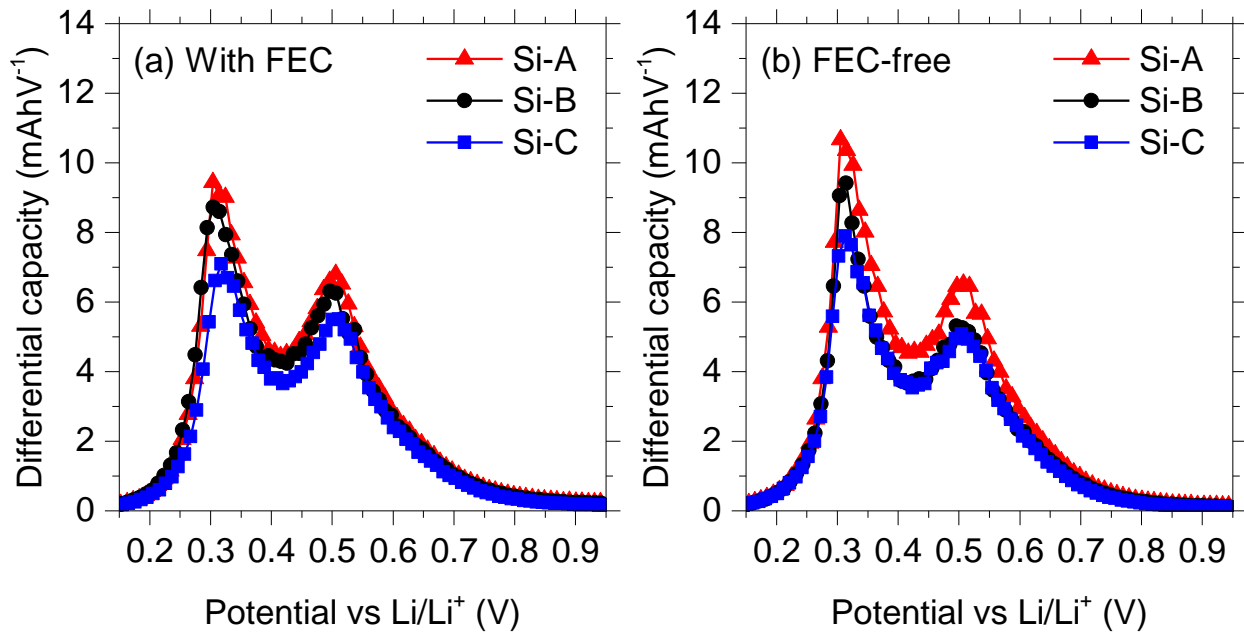


**Figure S9.** Differential capacity ( $dQ/dV$ ) plots of the Si NP/Li half cells using (a) electrolyte with FEC; and (b) electrolyte without FEC at 0.5 C rate, showing the absence of the expected characteristic c-Li<sub>15</sub>Si<sub>4</sub> peak at 0.45 V vs. Li/Li<sup>+</sup>.

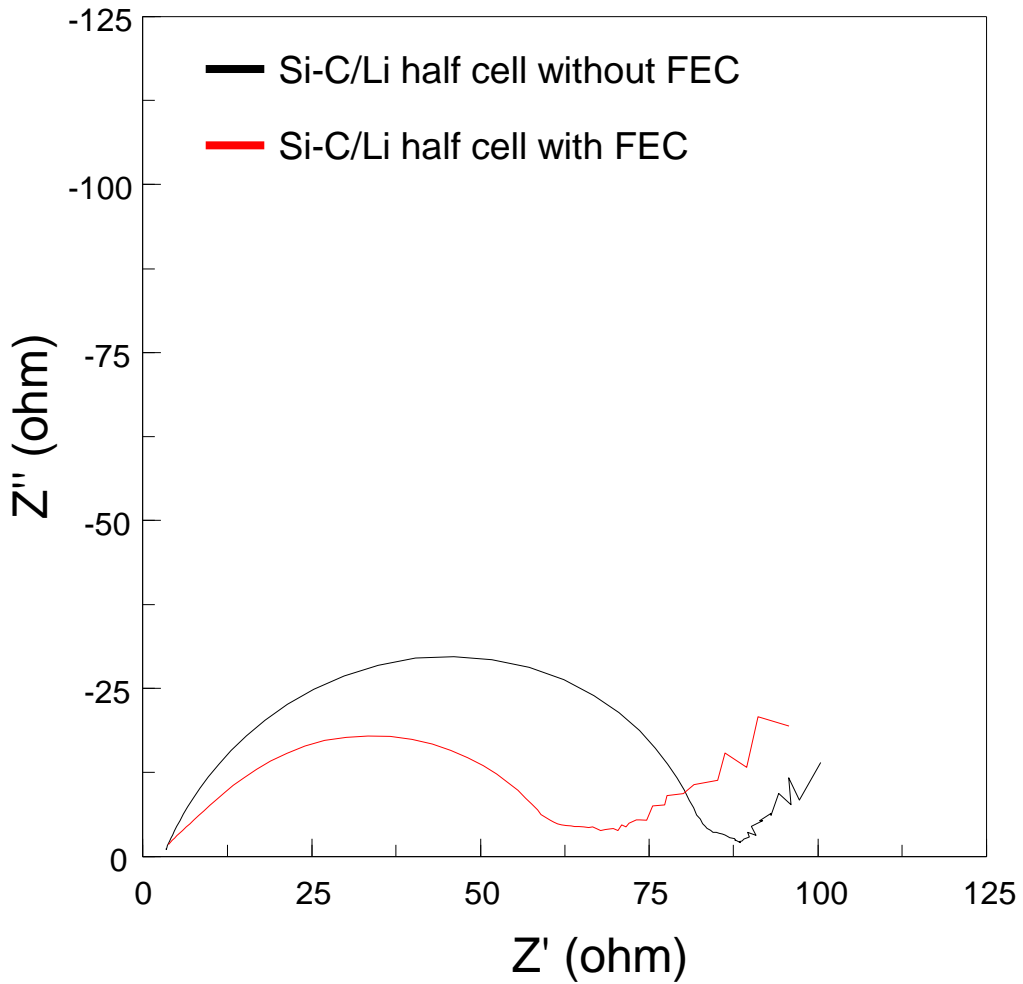


**Figure S10.** Nyquist plots of Si-C/Li half cells with and without FEC at 0 V vs. Li/Li<sup>+</sup> (2<sup>nd</sup> discharge, Frequency range = 100 kHz to 0.01 Hz, 10 mV amplitude).

**Table S1.** Brunauer-Emmett-Teller (BET) surface area of the three Si NP

Si NP	BET surface area ( $\text{m}^2\text{g}^{-1}$ )
Si-A	23.6
Si-B	30.0
Si-C	49.3

**References:**

1. Himpel, F. J.; McFeely, F. R.; Taleb-Ibrahimi, A.; Yarmoff, J. A.; Hollinger, G. *Physical Review B* **1988**, 38, 6084-6096.